CFD simulations of the transient response of a constant-temperature hot-wire anemometer

Serhat Yesilyurt
Sabanci University, Istanbul, Turkey
syesilyurt@sabanciuniv.edu

Meric Ozcan
Sabanci University, Istanbul, Turkey
meric@sabanciuniv.edu

Gokhan Goktug
Sabanci University, Istanbul, Turkey
ggoktug@sabanciuniv.edu

Hasan S. Olmez
Sabanci University, Istanbul, Turkey
olmez@sabanciuniv.edu

Abstract: *A numerical study of the transient response of a constant-temperature hot-wire anemometer is presented. We use a commercial software, FEMLAB, to solve the coupled partial-differential equations: 2D Navier-Stokes, energy, and the ordinary differential equation that governs the electronic circuit's voltage.. It is common to analyze the hot-wire's response using steady-state correlations for convection heat transfer from the wire. In this work, we replace the steady-state correlations of convection heat transfer with the direct computation of the 2D transient flow around the wire. Dynamic response of the whole system is demonstrated with the step and sine-wave velocity inputs as realistic simulations mimicking the actual operating conditions of the wire, where the fluctuating component of the possibly turbulent velocity is being measured in real experiments. Results of the CFD simulations are compared with analytical results obtained from a simple lumped ODE model that is used commonly in the analysis of hot-wires for steady-state operation and for transient response. It is observed that the transient effect of the convection is responsible for important dynamics, which is not included in the simple ODE model that uses a correlation for steady-state convection.*

Keywords:. *Hot-wire anemometer, CFD, unsteady convection, unsteady flow*

1. Introduction

Hot-wire anemometers are common devices used in local mean flow and fluctuating velocity measurements. They are made of thin, a few microns, metal wires such as Platinum, Tungsten or their alloys. The small size of these wires is desirable for their fast transient characteristics as well as for local measurements. The fast thermal transient of the wire is easily matched with the dynamics of the electronic circuit (Bruun 95, Comte-Bellot 98). The basic operation of hot-wires relies on the electronic control of the voltage applied to the wire. The heated wire is cooled down by the external flow. From the temperature of the wire and the voltage applied to it, one can measure the velocity of the flow at a desired sampling rate almost up to 100 kHz (Dantec Dynamics 04).

A constant-temperature hot-wire anemometer is one, for which the temperature is kept constant by adjusting the voltage. The resistance of the metal wire is a temperature dependent property. By carefully balancing the circuit, in which the wire consists of one of the resistances, one can achieve electronic control that automatically adjusts the voltage to keep the resistance, and the temperature constant (Bruun 95).

Electronic control of hot-wires has been well-studied, for example (Freymuth 67, 77, and 78) and (Perry 82). There is also a number of studies that focuses on the effect of the thermal transients of a one-dimensional wire, for example by (Morris and Foss 03). In this work, we present a coupled 2-dimensional transient model of the heat balance in the wire and the surrounding fluid, flow over the wire, and the circuit. The Fig. 1a displays the sketch of a typical hot-wire probe; the length of the probe is usually much large than its diameter, for example a millimeter vs. few microns. Due to this large aspect ratio, and to save on the computational cost –compared to a 3D model, a 2D model is sufficient to model the transient convection. Unlike the 1D model used in (Morris and Foss 03), our 2D model does not have the heat conduction effect to the structure. The only mechanism that is responsible for the removal of the heat from the wire is convection created by the flow, which is modeled by means of a steady-state heat transfer correlation in (Morris and Foss 03). The Fig. 1b displays the sketch of a computational domain considered here. To be specific, we use only the half domain and invoke the symmetry boundary condition at the line of symmetry to save on the computational cost.

The electronic circuit, which is shown in Fig 2., is modeled using a first order dynamics, which is commonly adopted by, for example Blackwelder 81, Jiang et al 94, Chen and Liu 03. The first-order dynamics of the electronic circuit, in particular the operational amplifier, is based on the wire's resistance which is a function of the averaged temperature of the wire. The voltage output of the circuit is used to calculate the volumetric heat generation in the wire due to Joule heating.

To study the transient effects on the circuit's voltage, which is the measured quantity in real experiments, we use the velocity as our input, unlike many electronic control and measurement work that rely on the electronic testing of the probe. Velocity perturbation, compared to voltage perturbation, is harder in real experiments, and hence somewhat less addressed; one example is the detailed experimental comparisons provided by Khoo et al (Khoo et al 99). In our work, voltage is computed in response to a step or a sine wave velocity input at the inlet. Details of the approach implemented here are provided in section 2, results in Section 3, and a conclusion and discussion in Section 4.
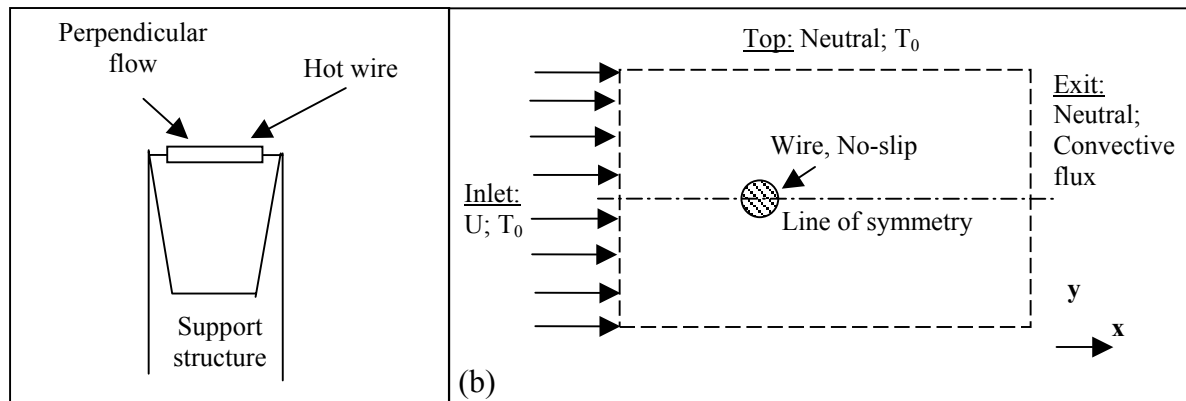

Figure 1: (a) A schematic view of a hot-wire probe; (b) 2-dimensional computational domain representing the flow over the wire and heat transfer, along with corresponding boundary conditions.

2. Model of the hot-wire anemometer

A variety of materials and geometries are used for hot-wire probes. As a representative, a 1 mm long Tungsten wire with 10 μm diameter is used here. The working fluid is air, and only sub-sonic incompressible flows are considered. The Reynolds number for the flow over the wire is low, $O(1)$. The computational domain is a 200 by 100 μm^2 rectangle as shown in Fig. 1b. Table 1 shows the properties of the Tungsten wire and the air at room temperature used in our simulations.

Table 1. Selected material properties used in this work

Property	Tungsten (at 300 K)	Air (at 300 K)
Density, ρ (kg/m^3)	19300	1.177
Specific heat, c_p (J/kg-K)	132	1005
Thermal conductivity, k (W/m-K)	174	.0267
Viscosity, μ (kg/m-s)	-	.184 x 10^{-4}
Temperature coefficient of resistance, α	0.0036	-

The flow over the wire is governed by the Navier-Stokes equations:

$$\rho\left(\frac{\partial \mathbf{u}}{\partial t} + \mathbf{u} \cdot \nabla \mathbf{u}\right) = -\nabla p + \mu \nabla^2 \mathbf{u} , \tag{1}$$

subject to the incompressibility condition:

$$\nabla \cdot \mathbf{u} = 0 ; \tag{2}$$

where ρ is the fluid's density, μ is viscosity, p is pressure, **u** is velocity vector, and t is time. The boundary conditions listed in Fig. 1b are: constant velocity in the x direction at the inlet, no-slip at the wire's perimeter, and neutral at the exit and at the top away from the wire; neutral boundary condition is the following:

$$\mathbf{n} \cdot \left[p\mathbf{I} + \mu \left(\nabla \mathbf{u} + \left(\nabla \mathbf{u} \right)^T \right) \right] = 0 \qquad (3)$$

where **n** is the surface outward normal, and **I** is the identity tensor. This boundary condition is useful for representing flow conditions that are minimally constrained (FEMLAB, 2004). In the flow direction, it ensures that the flow is well developed, and may exit the domain without any resistance or backflow; in the **y**-direction, sufficiently away from the cylinder, the neutral boundary condition ensures that flow may continue uniformly. In the model presented here, not only the computational domain is kept sufficiently large for a low Reynolds number flow, but also no-stress boundary conditions invoked to ensure a negligible interference due to the truncation of the flow domain.

The energy equation governs the conduction-convection in the fluid, and conduction in the fluid, and given by:

$$\rho^{(1,2)} c_p^{(1,2)} \left(\frac{\partial T}{\partial t} + \mathbf{u} \cdot \nabla T \right) = \nabla \cdot k^{(1,2)} \nabla T + Q \qquad (4)$$

where superscripts 1 and 2 correspond to the properties of the fluid and solid media respectively, c_p is the specific heat, k is the thermal conductivity, **u** is calculated from (1) and (2) in the fluid, and is zero in the solid; lastly Q is the heat generation source term given by:

$$Q(\mathbf{x}) = \begin{cases} 0, & \mathbf{x} \in \Omega_1 \\ \dfrac{4V^2 R}{\left(R + R_1 \right) \pi D^2 L}, & \mathbf{x} \in \Omega_2 \end{cases}, \qquad (5)$$

where $\Omega_{1,2}$ correspond to fluid and solid (wire) domains respectively, V is the output voltage, R is wire's resistance, R_1 is a circuit element (see Fig. 2), D wire's diameter, and L its the length. The temperature boundary conditions applied to the computational domain are displayed in Fig. 1b: at the inlet and the top, temperature is 0 (reference temperature); at the exit, the convective flux $\mathbf{n} \cdot \left(-k\nabla T \right)$ is set to zero, which ensures minimal influence of the exit conditions due to the truncation of the computational domain. The resistance of the Tungsten wire is temperature dependent, and can be approximated by linear interpolation for small temperature ranges:

$$R = R_0 \left(1 + \alpha \left(T - T_0 \right) \right), \qquad (6)$$

where R_0 is the resistance of the wire at the reference temperature T_0, and α is the temperature coefficient of the resistance at T_0.

For the electronic control of the constant-temperature hot-wire anemometer, a typical circuit is shown in Fig. 2 (Freymuth 77, Chen and Liu 03). Variations on the architecture of this circuit have been studied from electronic control point of view elsewhere. In this work, a simple circuit that provides the necessary first-order dynamics is used. The operational amplifier in the system, typically, is responsible for balancing the circuit and providing the necessary voltage for the operation of hot-wire at constant temperature, and resistance. The ordinary differential equation that governs the opamp's output is, typically, given by (Freymuth 77, Chen and Liu 03):

$$\tau \frac{dV}{dt} = - \left(AV - V_{off} \right), \qquad (7)$$

where τ is the time-constant of the opamp, V_{off} is the base voltage applied to the circuit, and A is a coefficient that encapsulates the elements of the circuit including the wire: $A = 1 - G\left(R_1 - R \right) / \left(R_1 + R \right)$, where G is the amplifier's gain.

In this study, transient response of hot-wire is determined by simultaneous (coupled) solution of equations (1), (4) and (7) with respect to the control variable, input velocity.

3. Numerical solutions

The PDE's (1) and (4) are solved in the computational domain depicted in Fig. 1b by invoking the multiphysics feature of the code (FEMLAB 2004); coupling of the convection-diffusion and the Navier-Stokes equations is straightforward. As its name suggests, FEMLAB uses finite-elements; in this work second-order Lagrangian elements are used for discretization, and FEMLAB's implicit algorithm is employed for time-stepping. Equation (7), which is an ODE, is formulated in FEMLAB using the weak PDE equation mode, which is invoked for only a single point at the

center of the wire, as suggested by the code's manual(FEMLAB 2004a). The solid and fluid media are triangulated with FEMLAB's own mesh generator. A typical mesh used in simulations is shown in Fig. 3.

Transient simulations are performed from various initial conditions. A typical final (steady-state) temperature distribution is shown in Fig 4. At constant velocity input, steady-state is reached within milliseconds, which is about the thermal time-constant, as discussed later in the section.
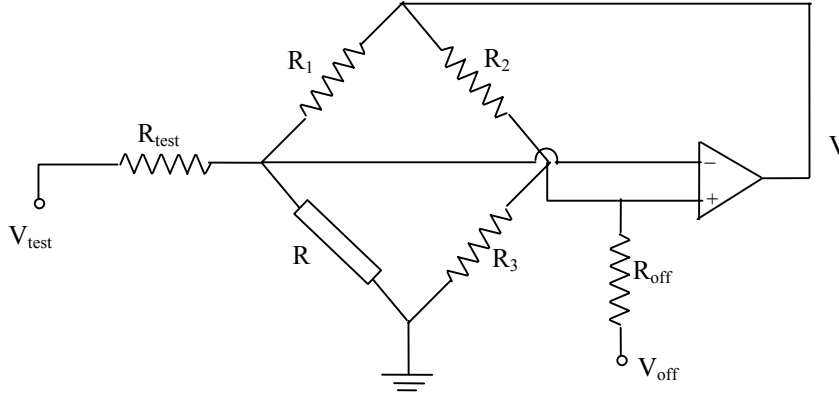

Figure 2: A schematic view of the electronic control circuit, R corresponds to the resistance of the hot-wire, V_{test} is for electronic testing (in this work set to 0), V_{off} is and offset voltage for opamp to output non-zero voltage, $R_{in} \gg R_1$, $R_2 = R_3$, and $R_{off} \gg R_1$.

Steady-state voltage against the input velocity is shown in Fig 5. This curve represents a typical calibration curve utilized in experimental studies. For the steady-state response of the anemometer, a simple relationship between the voltage and the flow velocity can be established by utilizing the conservation of energy, given in the form:

$$hA_w\left(T_w - T_f\right) = QV_w, \tag{8}$$

where, h is the convection coefficient; A_w is the surface area, V_w is the volume, and T_w is the average temperature of the hot-wire; T_f is the temperature of the fluid; and Q is given by (5). Heat transfer coefficient, h, can be calculated from the heat transfer correlation given by (Bruun 95):

$$\frac{hD}{k} = Nu = .42\,\mathrm{Pr}^{.26} + .57\,\mathrm{Pr}^{.33}\,\mathrm{Re}^{.45}, \tag{9}$$

where, D is the diameter, k is the thermal conductivity of air; and Pr and Re are the Prandtl, which is constant, .69 at 300 K, and Reynolds numbers. By substituting the Reynolds number, ($\rho UD/\mu$), in (9), and (9) and (5) in (8), we get the following relation for the voltage against the flow velocity:

$$V = \left[\pi LRk\Delta T\left(C_1 + C_2 U^{.45}\right)\right]^{.5}, \quad C_1 = .42\,\mathrm{Pr}^{.26}, \quad C_2 = .57\,\mathrm{Pr}^{.33}\left(D/\nu\right)^{.45}, \tag{10}$$

where, R is the resistance; L, length; k, thermal conductivity and and ν is the kinematic viscosity of air; and ΔT is, in effect, wire's average temperature, when the fluid's reference temperature is set to 0. Comparison of the lumped energy balance vs. the simulation results is shown in Fig 5. For the simulations performed here (U=1 to 15 m/s) the average temperature of the wire changes minimally from 320.75 K for U = 1 m/s to 320.5 for U = 15.
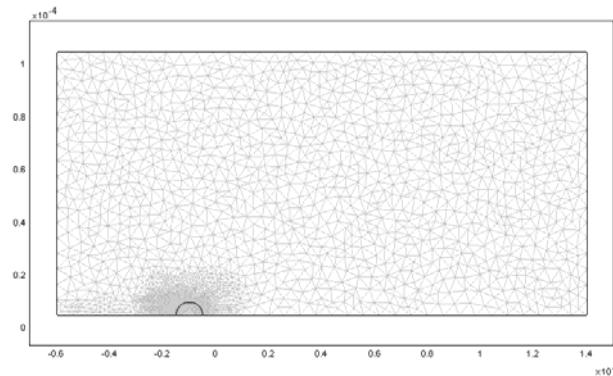
Figure 3: Triangulation of the solid and fluid domains: 5031 elements, 31487 d.o.f.

Hot-wire's response to a step change in the velocity is shown in Fig. 6, and compared to a simple lumped model widely used in calibration of the hot-wires. Lumped model uses the simple heat-balance for the wire, which is given by:

$$mc_p \frac{dT_w}{dt} = -hA\left(T_w - T_f\right) + QV_w,$$ (11)

where m is the wire's mass, and c_p its specific heat. Note that, to compare with our 2D CFD simulations, we only consider convection heat loss from the wire. In the lumped model, (11) and (7) constitute a second-order nonlinear system of equations, which is coupled by means of (5) and (6). The characteristic oscillations of the second order system are clearly seen in Fig. 6 in the lumped model's response. However, the response of the PDE system computed by the simulations does not have the characteristic second-order behavior. The closeness of the rise times and the maximum overshoots for the two ensures that the time constants of the two models are very close. Also note that the error in the steady state values of the two solutions is less than 1% (see also Fig. 5). The difference between the dynamic response of the lumped ODE model and the PDE model, in effect, hints that the damping in the detailed PDE model, which captures the full transient convection, is not included in the lumped ODE model.

The frequency response of the output voltage is shown in Fig. 7. For this analysis, we applied a sinusoidal input velocity in the range of 4.5 to 5.5 m/s, and calculated the gain in the output voltage. For low frequencies the gain, which is defined by, $20*\log(\Delta V_\omega/\Delta V_{DC})$ approaches to zero; where ΔV_{DC} is the output voltage difference for steady state values of 4.5 m/s and 5.5 m/s, and ΔV_ω is the range of the steady-periodic voltage output in response to the sine wave input. Consistently with the results in Fig. 6, the PDE model exhibits that it is **damped** considerably more compared to the ODE model. That effect is somewhat more emphasized here. Even though the ODE model results show that the voltage output is amplified more than 10^3 times near 3 kHz, numerical solutions to the PDE model do not follow that trend. Unfortunately, the computational requirements for numerical simulation are somewhat restrictive to compute the response of the PDE model in higher frequencies than about 1 kHz to further confirm that discrepancy.
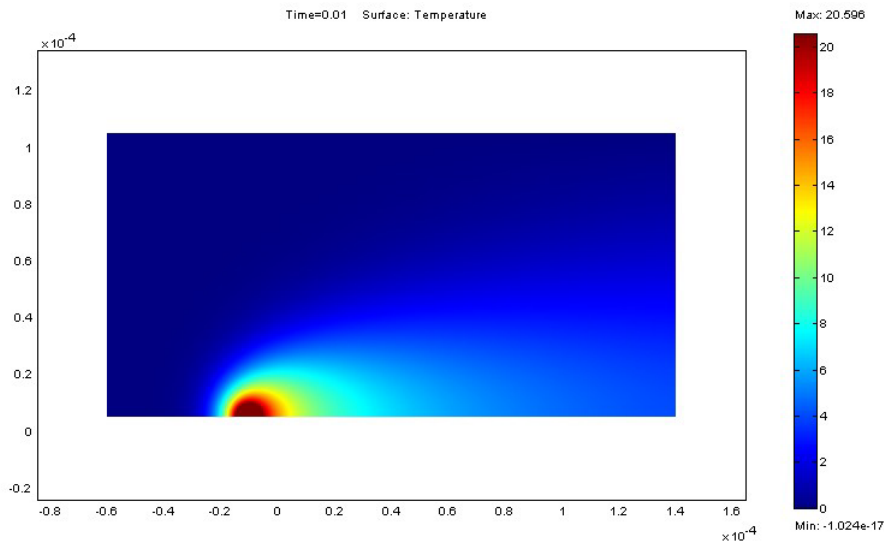
Figure 4: Final (steady-state at t = 0.01 s) temperature distribution in the flow surrounding hot-wire.

4. Conclusion

It is clear that albeit useful for the steady state analysis, simple lumped ODE models cannot adequately describe the full dynamics of a hot-wire anemometer, which has comparable time-scales for the thermal and electronic responses – here the electronic time scale is 2e-5 s and thermal time scale is on the order of 1e-3 depending on the flow velocity. Our results indicate that transient in the convection between the wire and the surrounding flow plays a very important role. We think that the convection term, $\mathbf{u} \cdot \nabla T$ in eq. (4) contains important dynamics that cannot be included in the lumped model, in eq. (11). In the lumped model convection is treated statically by means of the steady-state heat transfer coefficient, h. Hence the dynamics of the two models are very different.

For better design and operation of hot-wire anemometers, CFD tools prove useful. Especially for reliable measurement of the fluctuating component of the velocity, detailed analyses as presented here can be used effectively. Yet, our results here need to be verified with experimental results, first, and further modeling efforts can be deployed to study the effects of the natural convection, probe's heat loss to the support structure by conduction and to environment by means of radiation.
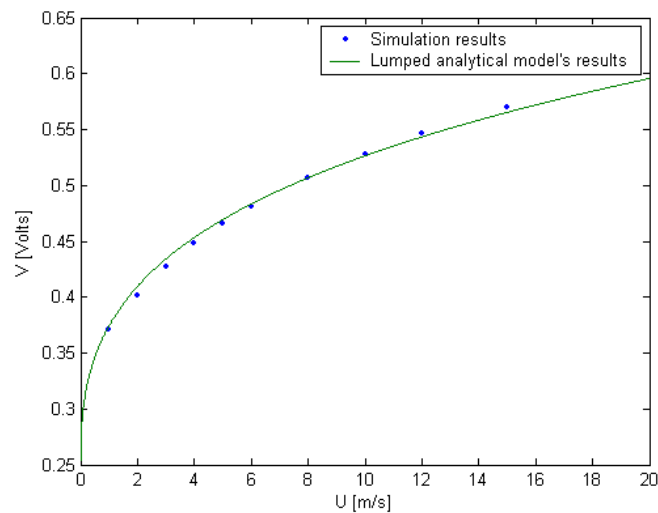

Figure 5: Steady-state results: simulations (blue dots) vs. the lumped analytical model given by (10).
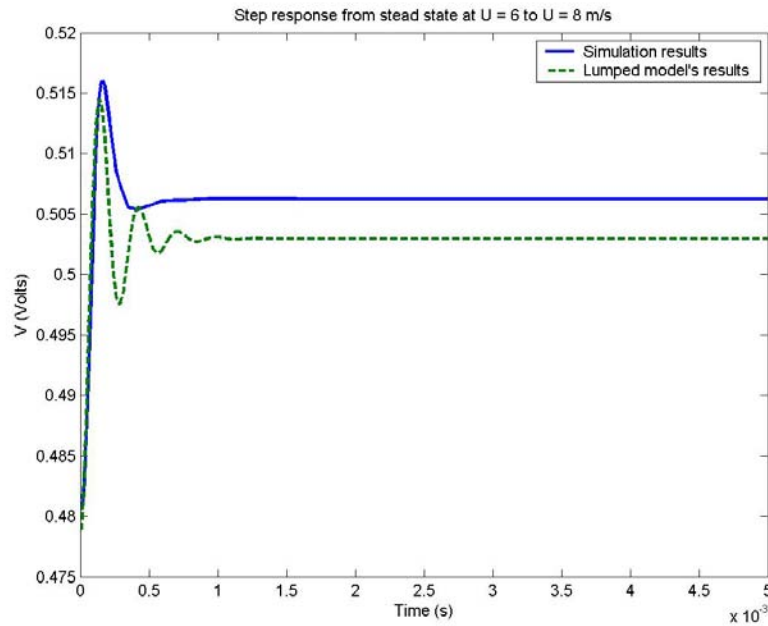
Figure 6: Response of the circuit's voltage (initially at steady-state) to a step change in the velocity from U=6 to 8 m/s: solid line corresponds to our numerical results, and the dashed line corresponds to the simple lumped model given by (7) and (11).
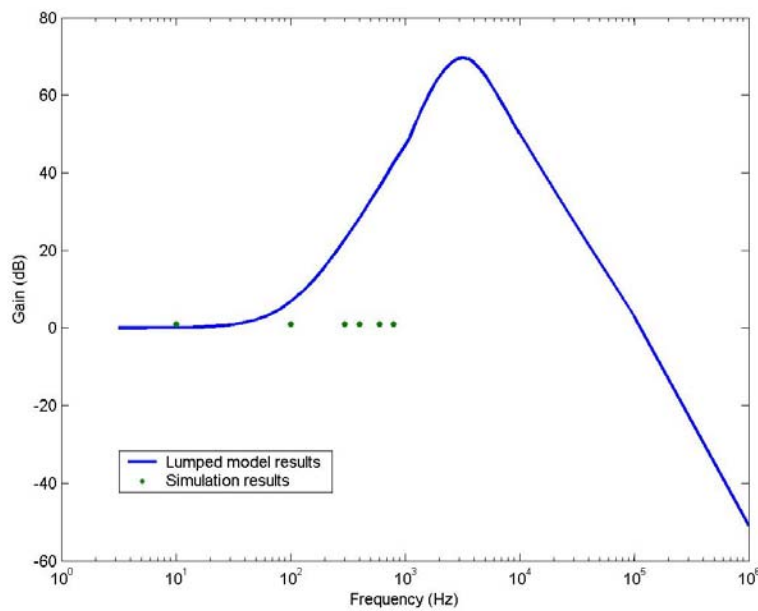

Figure 7: Frequency response of the anemometer, where gain is given by $20*\log(\Delta V_\omega/\Delta V_{DC})$.

5. References

Blackwelder, R.F., 1981, "Methods of Experimental Physics: Fluid Dynamics", Vol 18, Part A, Academic Press, pp. 259-314.

Bruun, H. H., 1995, "Hot-wire anemometry: Principles and Signal Analysis", Oxford University Press, New York.

Chen, J., and Liu, C., 2003, "Development and characterization of surface micromachined, out-of-plane hot-wire anemometer", J. Microelectromechanical Systems, Vol 12, No. 6, pp. 979-988.

Comte-Bellot, G., 1998, "Handbook of Fluid Mechanics", CRC Press, Boca-Raton, FL.

Dantec Dynamics, 2004, "Product Catalog", http://www.dantecdynamics.com

FEMLAB 2004, "FEMLAB 3.0 Modeling Guide", Comsol AB, Stockholm.

FEMLAB 2004a, "FEMLAB 3.0a, Multidisciplinary models", Comsol AB, Stockholm.

Freymuth, P., 1967, "Feedback control theory for constant-temperature hot-wire anemometers", Rev. Sci. Instrum., Vol. 38, pp. 677-681.

Freymuth, P., 1977, "Frequency response and electronic testing for constant-temperature hot-wire anemometers", J. Phys E: Sci. Instrum., Vol. 10, pp. 705-710

Freymuth, P. 1978, "Theory of frequency optimization for hot-film anemometers", J. Phys. E: Sci. Instrum., Vol. 11, 177-179.

Jiang, F., Tai, Y.C., Ho, C.M., Karan, R., and Garstenauer, M, 1994, "Theoretical and experimental studies of micromachined hot-wire anemometers", Technical Digest, International Electron Devices Meeting, San Fransisco, pp. 139-142.

Khoo, B.C., Chew, Y.T., Lim, C.P., and Teo, C.J., 1999, "Dynamics response of a hot-wire anemometer. Part III: Voltage-perturbation versus velocity-perturbation testing for near-wall hot-wire/film probes", Meas. Sci. Technol., Vol 10, pp. 152-169.

Perry, A. E., 1982, "Hot-wire Anemometry", Oxford University, New York.

Morris, S.C., and Foss, J.F., 2003, "Transient thermal response of a hot-wire anemometer", Measurement Science and Technology, Vol. 14, pp. 251-259.